Cancer Chemother Pharmacol (2007) 59:711–723
DOI 10.1007/s00280-006-0325-3

ORIGINAL ARTICLE

Platinum drug effects on the expression of genes in the polyamine pathway: time-course and concentration-effect analysis based on Affymetrix gene expression profiling of A2780 ovarian carcinoma cells

Ram Varma · Suzanne Hector · William R. Greco · Kimberly Clark · Lesleyann Hawthorn · Carl Porter · Lakshmi Pendyala

Received: 18 May 2006 / Accepted: 7 August 2006 / Published online: 22 September 2006

Abstract
Purpose As a follow-up to our previous findings that platinum drugs induce a key enzyme in polyamine catabolism, gene expression profiling and mathematical modeling were used to define the effects of cisplatin and oxaliplatin on the expression of polyamine metabolic pathway genes in A2780 human ovarian carcinoma cells.
Methods Time-course and concentration–effect experiments were each carried out with cisplatin or oxaliplatin in two separate experiments and cells subjected to gene expression profiling using Affymetrix array technology. Time-course data were modeled using exponential increase and decrease models. Concentration–effect data were modeled using a four parameter Hill model.
Results Gene expression profiling of human ovarian carcinoma A2780 cells after exposure to either cisplatin or oxaliplatin indicates that the expression of several genes involved in polyamine pathway is affected by the platinum drugs. Mathematical/Statistical modeling of the data from time-course and concentration–effect experiments of gene expression from nine polyamine pathway genes represented on the HGU95Av2 chip, indicates that three biosynthetic pathway genes (SAMDC, ODC1 and SRM) are down-regulated and one catabolic pathway gene (SSAT) is up-regulated. Expression changes were similar for different probesets for a given gene on the array. Studies on the induction of SSAT by platinum drugs suggested by the Affymetrix data have been previously validated from this laboratory (Hector et al. in Mol Cancer Ther 3:813–822, 2004). Here, the effects of oxaliplatin exposure on SAMDC and ODC observed by Affymetix are validated with real time QRT-PCR.
Conclusion The data indicate a concerted effect of platinum drugs on the polyamine metabolic pathway with down-regulation in the expression of several enzyme genes involved in biosynthesis and many-fold up-regulation in expression of SSAT, an acetylating enzyme gene that is critically involved in polyamine catabolism and export.

Keywords Cisplatin · Oxaliplatin · Platinum · Polyamines · Gene expression profiling

Abbreviations

Put	Putrescine
Spd	Spermidine
Spm	Spermine
ODC1	Ornithine decarboxylase
SAMDC	*S*-adenosylmethionine decarboxylase
SSAT	Spermidine/spermine N^1-acetyltransferase (also known as SSAT-1)

R. Varma · W. R. Greco
Cancer Prevention and Population Sciences,
Roswell Park Cancer Institute, Buffalo, NY 14263, USA

S. Hector · K. Clark · L. Pendyala (✉)
Department of Medicine,
Roswell Park Cancer Institute, Buffalo, NY 14263, USA
e-mail: lakshmi.pendyala@roswellpark.org

L. Hawthorn
Cancer Genetics,
Roswell Park Cancer Institute, Buffalo, NY 14263, USA

C. Porter
Pharmacology and Therapeutics,
Roswell Park Cancer Institute, Buffalo, NY 14263, USA

SMS	Spermine synthase
SRM	Spermidine synthase
SMOX	Spermine oxidase
OAZ	Ornithine decarboxylase antienzyme
OAZIN	Ornithine decarboxylase antienzyme inhibitor
MTA	Methylthioadenosine
AcCoA	Acetylcoenzyme A
DENSPM	N^1N^{11}-diethylnorspermine
QRT-PCR	Quantitative RT-PCR

Introduction

The platinum drugs cisplatin and oxaliplatin are central to many cancer chemotherapy regimens today. All platinum drugs bind readily to DNA, RNA, protein and many small molecules in the cells [4]. However, it is widely believed that it is the formation of Pt-DNA adducts that leads to cytotoxicity of platinum drugs [4, 11]. Preliminary analysis of our Affymetrix gene expression data of A2780 cells treated with cisplatin or oxaliplatin indicated that platinum drugs affect the expression of hundreds of genes, representing DNA damage response, cell cycle, apoptosis, DNA repair, various signal transduction pathways and some metabolic pathway genes including those in the polyamine pathway [14].

The essentials of polyamine metabolism are shown in Fig. 1. The polyamines putrescine (Put), spermidine (Spd) and spermine (Spm) are organic cations, essential for cell proliferation [28]. Pharmacological or genetic depletion of cellular polyamines especially Spd invariably results in the inhibition of growth [8, 19, 24, 35]. Because they are positively-charged at physiological pH, polyamines bind electrostatically with negatively-charged macromolecules such as DNA and RNA, and thus, they have been implicated in stabilization of nucleic acids [28]. The requirement for cell growth is typically met by a biosynthetic pathway regulated by ornithine decarboxylase (ODC) and *S*-adenosylmethionine decarboxylase (SAMDC) and balanced by a polyamine catabolic pathway regulated by spermidine/spermine N^1- acetyltransferase (SSAT). The activity and turnover of the key biosynthetic enzyme ODC is controlled by a family of ODC anti-enzymes (antizymes; OAZ) [20]. In response to polyamine excess and certain other stimuli, OAZ binds to ODC and brings about inactivation of the enzyme by targeting it for a ubiquitin-independent process of degradation [20]. The ODC antizyme inhibitor (OAZIN) is a homolog of ODC which binds OAZ and thereby inhibits degradation of ODC [16]. Thus, the ODC activity and the down-stream polyamine biosynthesis are regulated by the antizyme and the antizyme inhibitor [16, 20]. On the catabolic side, the enzyme reaction catalyzed by SSAT represents the rate-limiting event. Acetylation of Spm and Spd by SSAT alters the net positive charge of those molecules and thereby facilitates either export out of the cell [31] or recognition for oxidation by polyamine oxidase (PAO) [36] and their back-conversion to Spd and Put, respectively, events that serve to lower the total intracellular polyamine pool. A newly discovered eukaryotic enzyme spermine oxidase (SMOX) catalyzes the direct oxidation of Spm to Spd and hence, bypasses the acetylation step required for back-conversion via PAO [10, 34].

The polyamine metabolic pathway is of particular interest since it has been shown that polyamine biosynthetic enzyme activity (i.e. ODC) and the levels of polyamines are higher in tumor cells than in normal cells as described for colon, prostate and breast cancers [6, 21, 22]. Because both polyamine biosynthesis and catabolism are oppositely regulated by intracellular polyamine pools, polyamine analogs can be used to down-regulate biosynthesis and potently up-regulate polyamine catabolism, thereby achieving rapid pool depletion and growth inhibition. This strategy has been adapted in the development of the polyamine analog N^1,N^{11}-diethylnorspermine (DENSPM) which continues to undergo clinical evaluation [29]. As noted above, acetylation of polyamines by SSAT leads to their catabolism and export and hence to polyamine depletion in the cells. Experimental approaches relying on analog up-regulation of SSAT, genetic manipulation such as siRNA knockdown of SSAT or conditional over-expression of SSAT, all suggest that induction of SSAT promotes growth inhibition and/or apoptosis in various human tumor cell models [8, 29, 35]. For example, a close correlation between SSAT induction and growth inhibition within a panel of human tumor cell lines that differentially induce the enzyme in response to a polyamine analog DENSPM has been described [24, 27]. Similar correlations were noted with analogs that differentially induced the enzyme in the same cell line [17]. Importantly, studies demonstrating the antitumor activity of DENSPM in human melanoma xenografts in nude mice showed that SSAT induction in tumor was ~40 times higher than liver and ~10 higher than kidney [23]. Since SSAT is among the top 20 genes up-regulated by oxaliplatin and cisplatin, we have devoted considerable effort in demonstrating that platinum drug

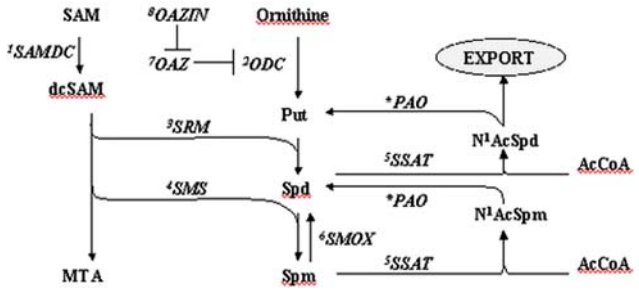

Fig. 1 Polyamine metabolic pathway. Polyamine biosynthesis (*left*) of Put, Spd, and Spm is co-regulated by pathway lead-in enzymes ODC and SAMDC while catabolism of polyamines is regulated by SSAT. These enzymes, in turn, are feed-back regulated by intracellular polyamine levels. In response to polyamine excess, OAZ binds to ODC, inhibits enzyme activity and targets the protein for degradation. OAZIN binds to OAZ and thereby inhibits the degradation of ODC. By contrast, SSAT is positively-regulated by Spd and Spm allowing the enzyme to counter intracellular polyamine excess which can be toxic. Following acetylation by SSAT, Spd or Spm are either exported out of the cell or degraded by polyamine oxidase (*PAO*). As an alternative to this back-conversion pathway, spermine oxidase (*SMOX*) can convert Spm to Spd without the prior need for acetylation. Genes for all the enzymes for the polyamine metabolic pathway shown in italics are represented on the Affymetrix HGU95Av2 chip. PAO (*asterisked*) is not on the chip. Abbreviations: *SAM S*-adenosylmethionine; *dcSAM* decarboxylaed *S*-adenosylmethionine; *MTA* methylthioadenosine; *Put* Putrescine; *Spd* spermidine; *Spm* spermine; *ODC1* ornithine decarboxylase; *SAMDC S*-adenosylmethionine decarboxylase; *SSAT* spermidine/spermine N^1-acetyltransferase (also known as SSAT-1); *SMS* spermine synthase; *SRM* spermidine synthase; *SMOX* spermine oxidase; *OAZ* ornithine decarboxylase antienzyme 1; *OAZIN* ornithine decarboxylase antienzyme inhibitor; *AcCoA* Acetylcoenzyme A. The number of probesets present on the chip for each gene are as follows: [1]SAMDC, 4 (262_at; 263_g_at; 36684_at; 36686_at); [2]ODC, 2 (1081_at; 36203_at); [3]SRM, 1 (241_g_at); [4]SMS, 1 (38792_at); [5]SSAT, 2 (34304_s_at; 1173_g_at, alternate splicing); [6]SMOX, 2 (1649_at; 1650_g_at); [7]OAZ1, 1 (1315_at); [7]OAZ2, 1 (36416_g_at); [8]OAZIN, 2 (1959_at, 33367_s_at)

induction of SSAT mRNA and activity in human ovarian carcinoma A2780 cells is causally related to growth inhibition [15]. Our studies indicated that while at clinically achievable concentrations and exposure times oxaliplatin induced high levels of SSAT mRNA and some SSAT activity, combining it with a clinically relevant polyamine analog DENSPM produces massive levels of mRNA and activity and depleted the polyamine pools [15]. Because SSAT is involved in polyamine catabolism, we evaluated the effects of platinum drugs on all the genes represented in polyamine metabolism on the Affymetrix U95Av2 chip in both time-course and concentration-effect experiments and are the focus of this paper. The results suggest a concerted effect on polyamine metabolism involving both induction of SSAT and down-regulation of biosynthetic enzyme genes.

Materials and methods

Drugs

Oxaliplatin was a gift from Dr. Paul Juniewicz of Sanofi-Synthelabo (Malvern, PA, USA). Cisplatin was purchased from Sigma Chemical Company (St. Louis, MO, USA).

Cell culture

A2780 is a human ovarian carcinoma cell line generously provided by Dr. Ozols (Fox Chase Cancer Center, Philadelphia, PA, USA). Cells were mycoplasma-free and maintained in RPMI 1640 supplemented with 10% fetal bovine serum (FBS) and 1% L-glutamine at 37°C in humidified 5% CO_2 atmosphere.

Cytotoxicity studies

Cytotoxicity measurements were carried out using the sulforhodamin-B micro-culture colorimetric assay [25]. Cells were exposed to either oxaliplatin or cisplatin for 2 h, washed and incubated in fresh medium for 70 h to estimate the IC_{10}–IC_{90} parameters for growth inhibition.

Time-course experiments

Cells were treated with IC_{90} concentrations of either oxaliplatin (32 μM) or cisplatin (25 μM) for 2 h, washed thoroughly with PBS and allowed to grow in fresh medium for up to 24 h. Cells were harvested and processed at the following times: before treatment, immediately after treatment (0 h), and at 2, 6, 16 and 24 h after treatment. Data were obtained from two time-course experiments conducted on separate days. Zero drug controls were collected at pretreatment, 0, 2, 6 and 16 h. Additional replicate data was also available from other experiments (concentration–effect experiment described below) for samples prior to treatment and at the 16 h time point. Samples were processed and hybridized to Affymetrix HGU95Av2 chips per Affymetrix protocol described below.

Concentration–effect experiments

Cells were treated with increasing concentrations (estimated IC_{10}–IC_{90} concentrations from equivalent growth experiments) of either oxaliplatin or cisplatin for 2 h, followed by incubation in drug free medium for 16 h. The cells were then harvested and processed according to Affymetrix protocol. The IC_{10}, IC_{25}, IC_{50},

IC_{75} and IC_{90} concentrations for cisplatin and oxaliplatin were 2.6, 4.0, 6.4, 12 and 25 μM and 2.8, 4.8, 8.5, 17 and 32 μM, respectively. The Affymetrix gene expression data were obtained from two concurrent concentration–effect experiments for each drug. Additional replicate data was also available from other experiments (time-course experiments described above) for control samples and samples treated with IC_{90} concentration for both drugs.

Affymetrix assays

Total RNA from cells (10–15 × 10^6 cells) was isolated using a Qiagen RNeasy kit (Qiagen, Inc., Valencia, CA, USA) according to specifications. Poly-A RNA was then isolated using a Qiagen Oligotex kit (Qiagen, Inc., Valencia, CA, USA) from ~50 μg total RNA and processed according to Affymetrix specifications (Affymetrix GeneChip Expression Analysis Manual, Affymetrix Inc., Santa Clara, CA, USA). Briefly, double stranded cDNA was synthesized from ~2.5 μg poly-A RNA using the Superscript Choice System (Invitrogen, Grand Island, NY, USA) followed by amplification and biotinylation by in vitro transcription reaction (BioArray High Yield Trascription Labeling Kit, Enzo Diagnostics, Farmingdale, NY, USA). At all steps, the quality of each sample was evaluated throughout using gel electrophoresis and spectrophotometry. The biotinylated RNA products were then purified, fragmented, hybridized to the Affymetrix Gene Chip arrays and scanned following streptavidin–phycoerythrin staining. The quality of each fragmented sample was assessed by hybridization to test chips. cRNAs passing quality checks were then hybridized to Affymetrix HG-U95Av2 GeneChips.

Data analysis

Probe level analysis

Probe level analysis was performed using the model based expression index (MBEI) calculation method of Li and Wong using dChip v1.3 software and the robust multiarray average (RMA) method using the Bioconductor package as previously described [33].

Models for analysis of time-course data

The time course data were analyzed using either model (1) or (2), which describe the increasing or decreasing effect of the drugs over time on the expression levels of various genes. For time course increases, the two-stage time-dependent model (1) was used for gene expression level with an initial constant value followed after a lag time by an exponential increase to an asymptotic final value.

$$\begin{aligned} &\text{For } t \leqslant t_0, \quad y = y_0, \\ &\text{For } t \geqslant t_0, \quad y = y_0 + a\left(1 - \exp\left(-\frac{\ln 2}{t_{1/2}} \times (t - t_0)\right)\right) \end{aligned} \tag{1}$$

where

- y gene expression level
- t time in hours. Treatment started at $t = -2$ h and stopped at $t = 0$ h. Data were recorded up to $t = 24$ h.
- y_0 initial gene expression level
- t_0 time lag before change in gene expression i.e. time at which expression level starts to change from the initial constant level
- a change in expression level from the initial to the final value, i.e. $a = y_{\text{final}} - y_0$. The absolute value of a is the maximum effect.
- $t_{1/2}$ half-life time constant. i.e. time from t_0 at which the expression level y of a gene has reached one-half of the maximum effect.

For time course decreases, the two-stage time-dependent model (2) was used with an initial constant value followed after a lag time by an exponential decrease to an asymptotic final value of zero. The three-parameter model (2) is easily derived from model (1) by letting $a = -y_0$. The symbols in model (2) have the same meanings as in model (1). For constant gene expression time courses, the simple model, $y = y_0$, was used.

$$\begin{aligned} &\text{For } t \leqslant t_0, \quad y = y_0 \\ &\text{For } t \geqslant t_0, \quad y = y_0 \times \exp\left(-\frac{\ln 2}{t_{1/2}} \times (t - t_0)\right) \end{aligned} \tag{2}$$

Model for analysis of concentration–effect data

A four parameter Hill model was used for the concentration–effect data. Model (3) for both excitatory and inhibitory responses is shown below. For genes that were not responsive to drug exposure, the simple model, $y = B$, was used.

$$y = B + (E - B) \times \frac{x^m}{c_{50}^m + x^m} \tag{3}$$

where

- y gene expression level
- x dose or concentration
- B background/baseline or minimum level of expression; for inhibitory responses, B is the level at infinite drug concentration; for excitatory responses, B is the level at zero drug concentration
- E maximum gene expression level; for inhibitory responses, E is E_{con} the control level when no drug is present; for excitatory responses, E is E_{inf} the asymptotic level at infinite drug concentration
- c_{50} the drug concentration that induces 50% of the maximum effect ($E - B$); for inhibitory responses, c_{50} is the IC_{50}; for excitatory responses, c_{50} is the EC_{50}. To facilitate the curve fitting procedure, K, the base 10 logarithm of the c_{50} was estimated directly, and the c_{50} was then calculated from K. Note that c_{50} was replaced by 10^K in model (3) for the actual curve fitting.
- m Hill sigmoidicity parameter; for inhibitory responses, m is negative; for excitatory responses, m is positive

Fitting of models to data

When fitting the models to the observed data, heteroscedasticity (lack of uniform dispersion) in measured gene expression levels was compensated for by weighting the data by the reciprocal of the estimated measurement variance. The measurement variance was proportional to the 1.71 power of the observed gene expression level [estimated from plotting the log(variance) against the log(mean) (not shown)] for replicates at each design point for the 16 probesets (9 distinct polyamine enzyme genes). The appropriate mathematical models described above were fitted to the experimental gene expression data first using SigmaPlot v. 9 (Systat, Inc., Point Richmond, CA, USA), and then SAS NLIN v. 9.1 (SAS Institute, Cary, NC, USA). SigmaPlot uses the Marquardt–Levenberg least squares algorithm for curve fitting; the Gauss–Newton algorithm option was used in SAS NLIN. A SigmaPlot macro was developed by Dr. Richard Mitchell (Systat Inc.,) during the course of this project to estimate model parameters for large number of probesets. The final parameter estimates, standard errors and fitted curves in this report are from the SAS results.

In general, the final nonlinear regression fits of the models to the data were required to have the 95% confidence intervals around their parameter estimates exclude the value zero, and to have the P value for the goodness of fit F-statistic be less than 0.0001. To accomplish this, for increasing time courses of gene expression, the time lag was fixed to be 2 h (the end of drug exposure), and the a parameter was fixed to the estimated value in the penultimate nonlinear regression run. For decreasing time-courses, only the time lag was fixed (to 2 h). Thus, only the y_0 and half-life parameters were formally estimated for both increasing and decreasing time courses. For concentration–effect curves, the m slope sigmoidicity parameter was fixed to the estimated value in the penultimate run. Thus, the Econ/Einf, B and K ($K = \log c_{50}$) parameters were formally estimated.

Polyamine pathway genes represented on the U95A chip

The interrelationships among the major enzymes and substrates in the polymaine pathway are shown in Fig. 1. The specific Affymetrix HGU95Av2 probesets corresponding to genes in the polyamine pathway are listed in the legend to Fig. 1. Several genes, including SSAT and SAMDC are represented by multiple probesets on the chip. Replicate probesets for the same gene showed similar results; only the results from one probeset per gene are included in this report.

Table 1 lists the probeset names for the representative examples of the nine genes included in this report.

Table 1 Correspondence among Probeset ID, gene name and gene symbol

Probeset ID	Gene name	Gene symbol
34304_s_at	Spermidine/spermine N1-acetyltransferase	SSAT
263_g_at	*S*-adenosylmethionine decarboxylase 1	SAMDC
1081_at	Ornithine decarboxylase 1	ODC1
38792_at	Spermine synthase	SMS
1315_at	Ornithine decarboxylase antienzyme 1	OAZ1
1959_at	Ornithine decarboxylase antienzyme inhibitor	OAZIN
36416_g_at	Ornithine decarboxylase antienzyme 2	OAZ2
1649_at	Spermine oxidase	SMOX
241_g_at	Spermidine synthase	SRM

Experiment to validate the effect of oxaliplatin on SAMDC and ODC

Real time QRT-PCR was carried out as described previously [15], on cells treated with oxaliplatin or cisplatin to confirm the effects of oxaliplatin and cisplatin on SAMDC and ODC Affymetrix microarray gene expression results. Cells were treated for 2 h at varying concentrations of the drugs, cells were washed free of drug, and then incubated in drug free medium for 24 h prior to the extraction of RNA. β-actin was the house keeping gene used as the internal standard. Primers and probes for SAMDC and ODC were purchased from Applied Biosystems Inc., as assay on demand kits. Comparative C_T method of quantitation was used as described previously [13]. The four-parameter Hill model (3) was fit to the QRT-PCR data with SAS NLIN. The weighting exponent was estimated to be 1.44 for this data. The final nonlinear regression runs had the B parameter fixed at 20% of the final Econ estimate; and the m slope sigmoidicity parameter fixed at the estimate from the penultimate run. Thus, only two parameters, Econ and K (log of IC50) were formally estimated from the data.

Results

Time course

Figure 2 and Tables 2, 3, 4 show the results from the analysis of the time course data. Figure 2 shows representative time-course plots with fitted curves for nine polyamine enzyme genes. Model parameter estimates (±SE), and the directions of change for these genes are shown in Tables 2, 3, 4. As evident from the results, three of the biosynthetic pathway genes (SAMDC, ODC1, SRM) show a trend towards decline while SSAT shows an increase with time. Of the three biosynthetic pathway genes that show a trend towards decline with time, SAMDC and ODC1 show the steeper declines (shorter half-lives). Note that the individual expression scales are different for the plots; this highlights the differences in magnitude of change for each individual gene. The differences in baseline levels of gene expression for the nine polyamine enzyme genes is especially clear in Table 4. ODC1 shows the greatest absolute decrease in expression activity over 24 h; SAMDC and ODC1 show similar percent decreases over 24 h; and SSAT shows the largest-fold

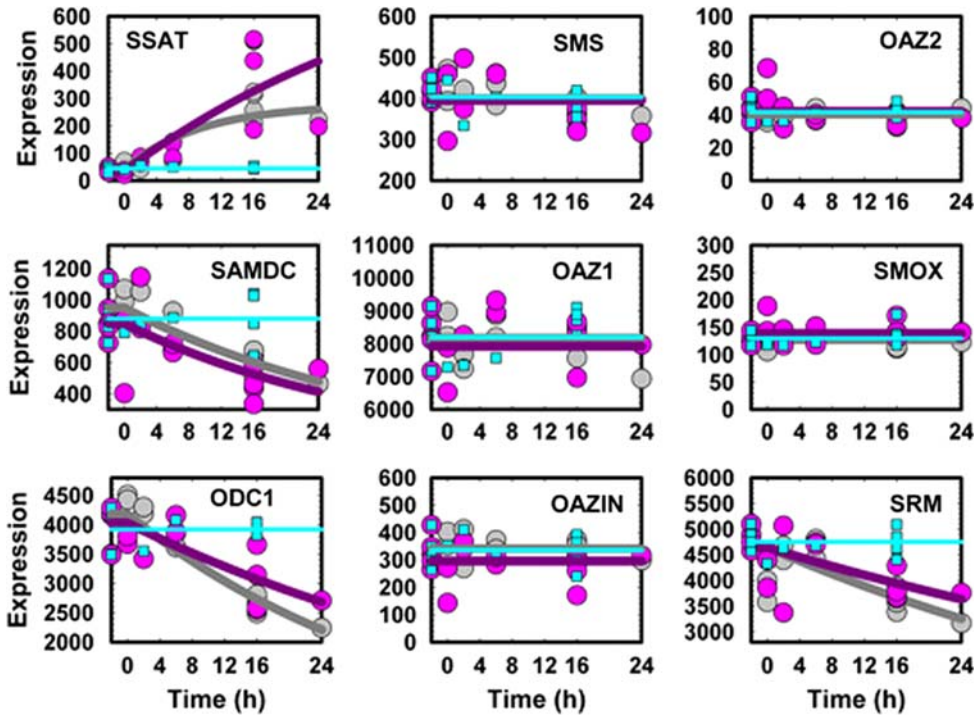

Fig. 2 Time courses for nine polyamine enzyme genes. The *y*-axes are gene expression in Affymetrix gene expression units; the *x*-axes are time relative to the end of the 2 h drug exposure (time 0) in hours. The *y*-axis scale is not the same for all genes; the *y*-axis has been scaled to best highlight the drug effect on each individual gene. The specific probe sets for each of the nine enzymes are listed in Table 1. The *gray circles* represent the gene expression data points for cisplatin exposure; the *gray curve* is the time course model fitted to this data as described in the text. The *pink circles* represent the data points for oxaliplatin exposure; the *pink curve* is the corresponding fitted time course model. The *blue squares* represent the data points for the control (no drug) exposure; the *horizontal blue line* is the average of these data points

Table 2 Final parameter estimates (±SE) for the fit of the cisplatin time course model to Affymetrix gene expression data

Gene symbol	Direction of change	y_0	a	Lag time t_0 (h)	Half-life $t_{1/2}$ (h)
SSAT	⇑	40.9 ± 8.3	237 fixed	2.00 fixed	6.42 ± 2.5
SAMDC	⇓	950 ± 40		2.00 fixed	24.3 ± 3.5
ODC1	⇓	4,180 ± 110		2.00 fixed	26.1 ± 2.4
SMS	⇔	400 ± 8.4			
OAZ1	⇔	8,170 ± 160			
OAZIN	⇔	341 ± 12			
OAZ2	⇔	40.5 ± 1.1			
SMOX	⇔	128 ± 2.8			
SRM	⇓	4,650 ± 140		2.00 fixed	46.7 ± 8.9

For the curve fitting, the lag time was fixed at 2 h after the beginning of the 2-h drug exposure (time 0 in Fig. 2)

y_0 initial expression level, a change in expression level from initial to the final value, i.e., $a = y_{\text{final}} - y_0$, $t_{1/2}$ time (h) to reach one half of the maximum effect from t_0, t_0 time lag; i.e., time (h) at which expression level starts to change

change in expression over 24 h (around a 12-fold increase for oxaliplatin and a 6-fold increase for cisplatin). Cisplatin and oxaliplatin appear to have similar effects to each other on the time course declines for SAMDC, ODC1 and SRM. Multiple probesets for the same gene for SSAT, ODC1, and SAMDC show consistently similar patterns and model fitted curves (data not shown), suggesting that the modulation of expression of these genes by oxaliplatin and cisplatin are indeed real. The intensity ranges for multiple probesets are different and possibly reflect differences in the actual target sequences and hybridization affinities. The profiles of induction of the SSAT gene by cisplatin and oxaliplatin are quite similar; any differences in parameter estimates may be due to a few aberrant data points. All control time courses, and the drug-induced time courses for SMS, OAZ1, OAZIN, OAZ2 and SMOX, appear to be steady over the 24 h time frame of this study. However, subtle time course patterns may be masked by data variation. Overall the coefficient of variation for replicate samples for these data was around 30%.

Concentration–effect

Figure 3 and Tables 5, 6 show the results from the analysis of the concentration-effect data; the data in Fig. 3 are for samples at 16 h after completion of a 2 h treatment at different doses of cisplatin (grey) or oxaliplatin (pink). Figure 3 shows representative concentration–effect plots with fitted curves for the same probesets as in Fig. 2 for the same nine polyamine enzyme genes. Model parameter estimates (±SE), and the directions of change for these genes are shown in Tables 5, 6. As evident from the results, three of the biosynthetic pathway genes (SAMDC, ODC1, SRM) show a trend towards decline with increasing concentration of drugs, while SSAT shows an increase with concentration. The exception to these general patterns is that oxaliplatin does not seem to alter the steady state level of ODC1 as seen by the model fitted curve. Of the three biosynthetic pathway genes that show a trend towards decline with time, SAMDC and SRM show the steeper declines (larger absolute values of the slope sigmoidicity parameter, m). Oxalipatin seems to be

Table 3 Final parameter estimates (±SE) for the fit of the oxaliplatin time course model to Affymetrix gene expression data

Gene symbol	Direction of change	y_0	a	Lag time t_0 (h)	Half-life $t_{1/2}$ (h)
SSAT	⇑	34.8 ± 6.3	908 fixed	2.00 fixed	28.5 ± 5.3
SAMDC	⇓	849 ± 69		2.00 fixed	23.1 ± 6.5
ODC1	⇓	4,030 ± 180		2.00 fixed	40.9 ± 11
SMS	⇔	395 ± 15			
OAZ1	⇔	7,920 ± 310			
OAZIN	⇔	296 ± 17			
OAZ2	⇔	42.1 ± 2.2			
SMOX	⇔	139 ± 4.9			
SRM	⇓	4,640 ± 160		2.00 fixed	68.2 ± 23

For the curve fitting, the lag time was fixed at 2 h after the beginning of the 2-h drug exposure (time 0 in Fig. 2)

Symbols are defined in the footnote to Table 2, and in the text

Table 4 Final parameter estimates (±SE) for the fit of the control (no drug) time course model to Affymetrix gene expression data

Gene symbol	Direction of change	y_0
SSAT	⇔	44.1 ± 2.6
SAMDC	⇔	881 ± 40
ODC1	⇔	3,920 ± 80
SMS	⇔	403 ± 9.9
OAZ1	⇔	8,200 ± 210
OAZIN	⇔	336 ± 17
OAZ2	⇔	41.7 ± 1.4
SMOX	⇔	130 ± 4.7
SRM	⇔	4,750 ± 75

Symbols are defined in the footnote to Table 2, and in the text

two- to fourfold more potent than cisplatin in affecting changes in SSAT, SAMDC and SRM (smaller EC50/IC50s). Note that the individual expression scales are different for the plots; this highlights the differences in magnitudes of changes for each individual gene. Cisplatin against ODC1 shows the greatest absolute decrease in expression activity (Econ-B); and SSAT shows the largest-fold change in expression (Einf/B) (around an eightfold increase for oxaliplatin and a ninefold increase for cisplatin). Cisplatin and oxaliplatin appear to have similar effects to each other on the time course declines for SAMDC and SRM; cisplatin seems to induce a decline in ODC1 expression, oxaliplatin does not seem to have an effect on ODC1 expression. Multiple probesets for the same gene for SSAT, ODC1, and SAMDC show consistently similar patterns and model fitted curves (data not shown), suggesting that the modulation of expression of these genes by oxaliplatin and cisplatin are indeed real. Similar to the time course results, the intensity ranges for multiple probesets are different and possibly reflect differences in the actual target sequences and hybridization affinities. The drug-induced concentration–effect patterns for SMS, OAZ1, OAZIN, OAZ2 and SMOX, appear to be steady over the concentration range for both agents used in this study. However, subtle concentration–effect patterns may be masked by data variation.

Validation of the effects of oxaliplatin and cisplatin on ODC and SAMDC by real time QRT-PCR

Under similar experimental conditions as described for Affymetrix experiments above (2 h drug exposure to

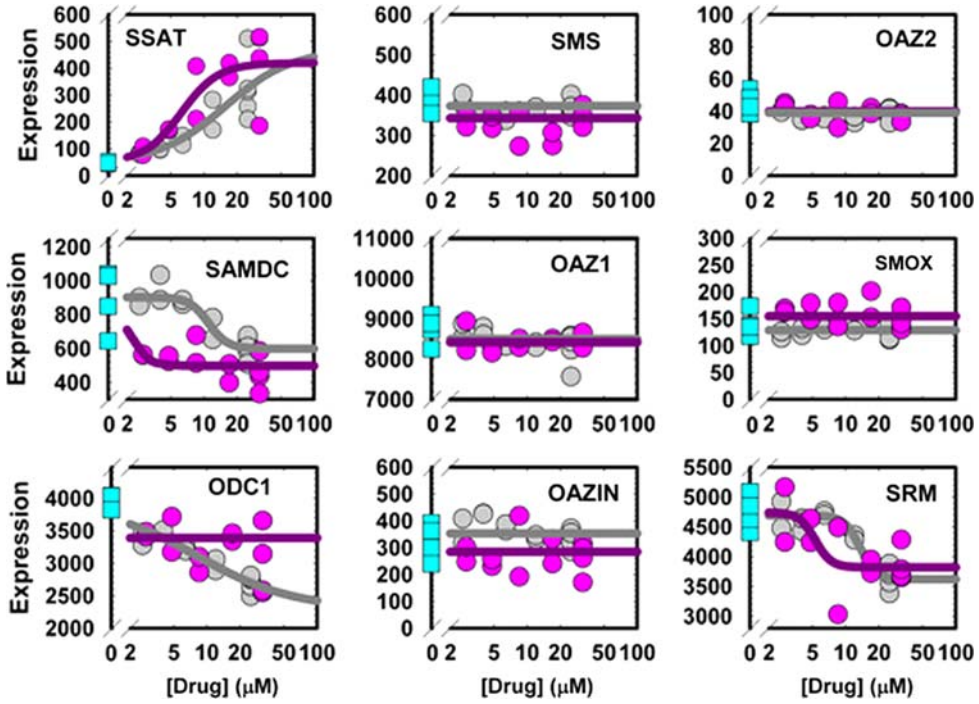

Fig. 3 Concentration–effect patterns for nine polyamine enzyme genes. The *y*-axes are gene expression in Affymetrix gene expression units; the *x*-axes are drug concentration in units of μM, on a logarithmic (base 10) scale. There is a break in the axis between the control samples and all of the drug-treated samples. The *y*-axis scale is not the same for all genes; the *y*-axis has been scaled to best highlight the drug effect on each individual gene. The specific probe sets for each of the nine enzymes are listed in Table 1. The *gray circles* represent the gene expression data points for cisplatin exposure; the *gray curve* is the concentration–effect model fitted to this data as described in the text. The *pink circles* represent the data points for oxaliplatin exposure; the *pink curve* is the corresponding fitted concentration–effect model. The *blue squares* represent the data points for the control (no drug) exposure

Table 5 Final parameter estimates (±SE) for the fit of the cisplatin dose response model to Affymetrix gene expression data

Gene symbol	Direction of change	Einf/Econ	*B*	*K* EC50/IC50 (μM)	*m*
SSAT	⇑	470 ± 100	49.0 ± 6.8	1.20 ± 0.15 15.8	1.44 fixed
SAMDC	⇓	903 ± 36	599 ± 37	1.04 ± 0.086 11.0	– 5.0 fixed
ODC1	⇓	3,920 ± 72	2,300 ± 150	0.914 ± 0.13 8.20	– 1.0 fixed
SMS	⇔		373 ± 5.8		
OAZ1	⇔		8,500 ± 84		
OAZIN	⇔		353 ± 12		
OAZ2	⇔		39 ± 1.0		
SMOX	⇔		129 ± 3.5		
SRM	⇓	4,690 ± 69	3,620 ± 84	1.13 ± 0.048 13.5	– 6.0 fixed

For the curve fitting, *m* was fixed at a value estimated in a preceeding run. The *K* parameter was actually estimated, and the EC50 or IC50 calculated from *K*

Einf the asymptotic level at very high concentration for an excitatory response, *Econ* control level at zero concentration for an inhibitory response, *m* Hill parameter (positive for excitatory response and negative for inhibitory response), *EC50* the drug concentration (μM) that induces 50% of maximum effect, *IC50* the drug concentration (μM) that inhibits 50% of the control, *K* logarithm (base 10) of either the EC50 or IC50, *B* lower control level at zero concentration for an excitatory response, or the lower asymptotic level at infinite concentration for an inhibitory response

IC_{10} to IC_{90} concentrations followed by sampling at 24 h), we carried out an evaluation of the effects of oxaliplatin and cisplatin on SAMDC and ODC gene expression in A2780 cells after treatment using real time QRT-PCR (Fig. 4, Table 7). Data shown are percent of expression after platinum drug treatment relative to the cells that were not drug treated (estimated E_{con} parameter). The four-parameter Hill concentration-effect model was fit individually to the four sets of data with SAS NLIN, with the background parameter, *B*, fixed at 20% of E_{con}, and the *m* slope sigmoidicity parameter fixed to the estimate from the penultimate run. As evident from the data and the fitted curves, both SAMDC and ODC expression decline in a sigmoidal manner with increasing concentrations of either oxaliplatin or cisplatin. Overall the coefficient of variation for replicate samples for these data was around 30–40%. The results are generally consistent with the Affymetrix results which showed a several-fold larger control gene expression activity for ODC over SAMDC (Tables 5, 6, 7) and IC_{50}s for oxaliplatin and cisplatin for both genes in the 1–20 μM range. Note that The QRT-PCR results show a clear concentration-effect pattern for oxaliplatin against ODC; whereas, the Affymetrix microarray results do not clearly show a pattern.

Table 6 Final parameter estimates (±SE) for the fit of the oxaliplatin dose response model to Affymetrix gene expression data

Gene symbol	Direction of change	Einf/Econ	*B*	*K* EC50/IC50 (μM)	*m*
SSAT	⇑	420 ± 41	49.0 ± 7.5	0.795 ± 0.061 6.24	2.56 fixed
SAMDC	⇓	890 ± 80	498 ± 32	0.315 ± 0.13 2.07	–5.0 fixed
ODC1	⇔		3,390 ± 120		
SMS	⇔		343 ± 11		
OAZ1	⇔		8,420 ± 120		
OAZIN	⇔		285 ± 17		
OAZ2	⇔		39.9 ± 1.2		
SMOX	⇔		155 ± 5.8		
SRM	⇓	4,740 ± 190	3,820 ± 140	0.723 ± 0.11 5.28	–6.0 fixed

For the curve fitting, *m* was fixed at a value estimated in a preceeding run. The *K* parameter was actually estimated, and the IC50 calculated from *K*

Symbols are defined in the footnote to Table 5, and in the text

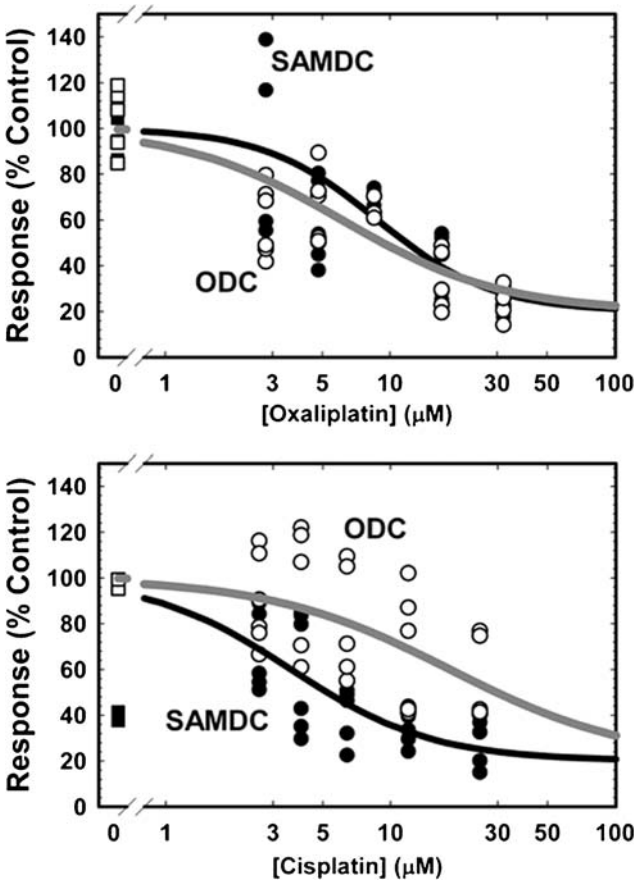

Fig. 4 Effect of oxaliplatin and cisplatin on SAMDC and ODC mRNA measured by RT-PCR. Cells were treated for 2 h with IC_{10} to IC_{90} concentrations of oxaliplatin or cisplatin, followed by incubation in drug free medium for 24 h prior to extracting the RNA. Data shown are percent expression relative to untreated controls. The fitted curves are from the fit of the four-parameter Hill model to the data as described in the text. The *filled symbols* are for SAMDC; the *open symbols* are for ODC (*square symbols* are for controls). The *thinner fitted black curve* is for SAMDC; the *thicker fitted gray curve* is for ODC. The *upper panel* is for oxaliplatin exposure; the *lower panel* is for cisplatin exposure

Discussion

With an aim to uncover previously unrecognized mechanisms of platinum drug action, we undertook an Affymetrix oligonucleotide array analysis of A2780 ovarian carcinoma cells exposed to oxaliplatin or cisplatin. These studies showed that a 2 h exposure to oxaliplatin or cisplatin results in a ≥ 2 fold change in up- or down-regulation of >200 genes at two or more time points during a 24 h period following the initial exposure [14, 32]. The altered expression is progressive with time, reaching a maximum at 16–24 h for a majority of the genes [14, 32]. Genes with altered expression at 16 h for either or both of the drugs included those related to DNA damage response (e.g., p21↑, GADD45↑, mdm2↑, BRCA1↓), cell cycle progression (e.g., p21↑, cyclin E2↓, cyclin A2↓), apoptosis (e.g., BID↓, caspase 6↑, caspase 10↑, Fas/Apo-1↑) and DNA repair (e.g., XPC2↑, ERCC-5↑, BRCA1↓, BRCA2↓) [32]. Changes in signal transduction pathways included Ras/MAPK, TGF beta receptor signaling, protein kinases and phosphatases. Expression of many metabolic pathway genes was also altered by platinum drugs, most notably SSAT, the polyamine acetylating enzyme. It was among the top 10 genes up-regulated by oxaliplatin and the top 20 genes up-regulated by cisplatin.

The effects of platinum drugs on SSAT and SMOX, the catabolic pathway enzymes, have been studied in greater detail by our laboratory and the findings have been published [15]. These previous studies [15] have shown that oxaliplatin is a potent inducer of SSAT mRNA in A2780 ovarian carcinoma cells and when combined with DENSPM, that induction can be synergistically increased. At pharmacologically-relevant concentrations and exposure times, induction of SSAT mRNA was 250-, 62- and 1.6-fold for the two-drug combination, oxaliplatin and DENSPM, respectively, while induction of SSAT enzyme activity was ~1,700-, 4- and 3.5-fold, respectively. Thus, DENSPM facilitates a massive conversion of SSAT mRNA to enzyme activity, presumably at the level of protein translation. Synergistic induction in SMOX mRNA was also observed with the two-drug combination, but to a smaller degree; oxidase mRNA was induced 7-fold by oxaliplatin, 2.5-fold by DENSPM and 16-fold by oxaliplatin and DENSPM. This super-induction of SSAT activity by the two-drug combination resulted in near total depletion of Spm and Spd; an event typically associated with growth inhibition. This study also showed that addition of a low dose DENSPM sensitized A2780 cells to oxaliplatin [15]. Since other polyamine pathway genes, including those from the biosynthetic pathway, are represented on the gene chip used in these studies, we went on to characterize the effect of platinum drugs on the expression of all of them, using rigorous mathematical/statistical modeling.

The time-course and concentration–effect profiling data presented in this paper show that platinum drugs not only induce the expression of the polyamine catabolic enzyme SSAT, but also down-regulate the expression of the polyamine biosynthestic enzyme genes SAMDC, ODC and SRM. It is reasonable to assume that the one contrary result of a lack of oxaliplatin concentration–effect pattern for the ODC Affymetrix probesets is an aberrant finding because of the high dispersion in Affymetrix data points. Polyamines have been implicated in the growth of cancer cells. The polyamine levels as well as the levels of ODC and

Table 7 Final parameter estimates (±SE) for the fit of the oxaliplatin and cisplatin concentration–effect models to QRT-PCR gene expression data

Gene symbol	Drug	Direction of change	Econ	*B*	*K* EC50/IC50 (μM)	*m*
SAMDC	Oxaliplatin	⇓	197 ± 20	39.3 fixed	0.945 ± 0.11 8.81	–1.71 fixed
ODC	Oxaliplatin	⇓	1,050 ± 110	211 fixed	0.788 ± 0.14 6.13	–1.22 fixed
SAMDC	Cisplatin	⇓	472 ± 150	94.4 fixed	0.557 ± 0.31 3.61	–1.38 fixed
ODC	Cisplatin	⇓	720 ± 68	144 fixed	1.27 ± 0.19 18.4	–1.07 fixed

For the curve fitting, *m* was fixed at a value estimated in a preceeding run. *B* was fixed at Econ/5. The *K* parameter was actually estimated, and the IC50 calculated from *K*

Symbols are defined in the footnote to Table 5, and in the text

SAMDC have been shown to be elevated in tumor cells compared to their normal counterparts [5, 22, 26]. Interference with the polyamine biosynthesis pathway as a means to inhibit cancer cell growth was the goal of earlier clinical studies with agents such as α-difluoromethyl ornithine [1]. It was subsequently recognized that inducing polyamine catabolism may be more effective in inhibiting tumor cell growth and inducing apoptosis than the inhibiton of biosynthesis [7, 19]. Many bis(ethyl)derivatives of natural polyamines have been synthesized as inducers of SSAT and were tested successfully for their cytotoxicity both in vitro and in vivo against various cancer cell models and some went on to clinical testing [29]. Analogs such as DENSPM have been shown to potently induce polyamine catabolism and export through SSAT and also to down-regulate polyamine biosynthesis at the level of ODC and SAMDC [9].

It is quite interesting how platinum drugs, which have no structure similarities with polyamine analogs behave similarly in affecting the polyamine pathway at the level of gene expression. Molecular mechanisms underlying these effects still need to be determined. Our earlier work indicated that while oxaliplatin induced SSAT at the level of gene expression, combining oxaliplatin with DENSPM facilitated translation of SSAT mRNA into active protein in a synergistic fashion [15]. It remains to be determined whether the effects of platinum drugs on ODC and SAMDC gene expression translate to effects at the protein level. It also needs to be determined whether a synergistic effect exists between platinum drugs and DENSPM in down-regulating ODC and SAMDC as was found to be the case in the up-regulation of SSAT [15].

Time-course and concentration–effect experiments using microarrays are usually analyzed with standard techniques such as class comparisons or clustering methods [12, 30]. However, the design of this study, with two or more replicates at several time points and concentrations, allowed the fitting of appropriate, logical, common mathematical/statistical models to the data. Our modeling paradigm was not based on general statistical approaches such as linear regression or splines, but rather on nonlinear regression curve fitting of models with a long history of success in characterizing pharmacologic time courses and concentration–effect patterns, with the inclusion of parameters of biological interest and significance [18]. There are very few reports of the modeling of gene expression data with parametric time-course models [2, 3] and even fewer reports (perhaps no reports) with concentration-effect models, such as the ones used in this paper. Modeling the time-course and concentration-effect data provided valuable preliminary insights for the different probesets of each of the polyamine genes and also provided insights into the relative potency and behavior of the two platinum drugs in the up- or down-regulation of the polyamine pathway genes. The Affymetrix gene expression profiling clearly predicted the significant induction of SSAT by platinum drugs as measured by QRT-PCR in our previous study [15], the decline in gene expression for SAMDC and ODC by cisplatin and oxaliplatin (with the one already noted exception) in the current study, but did not predict for the induction by platinum agents observed for SMOX in our previous studies [15].

In conclusion, work reported here indicate that platinum drugs exert a concerted effect on the polyamine pathway, up-regulating the catabolic pathway enzyme SSAT and down-regulating the biosynthetic pathway genes SAMDC, ODC and SRM. The information should prove useful as rationale in the design of mechanism-based combinations.

Acknowledgment This Research was supported by NIH CA109619, NIH RR10742 and CA-16056.

References

1. Abeloff MD, Rosen ST, Luk GD, Baylin SB, Zeltzman M, Sjoerdsma A (1986) Phase II trials of α-difluoromethylornithine, an inhibitor of polyamine synthesis in advanced small cell lung cancer and colon cancer. Cancer Treat Rep 70:843
2. Almon RR, Dubois DC, Jin JY, Jusko WJ (2005) Pharmacogenomic responses of rat liver to methylprednisolone: an approach to mining a rich microarray time series. AAPS J 7:E156–E194
3. Almon RR, Lai W, Dubois DC, Jusko WJ (2005) Corticosteroid-regulated genes in rat kidney: mining time series array data. Am J Physiol Endocrinol Metab 289:E870–E882
4. Boulikas T, Vougiouka M (2003) Cisplatin and platinum drugs at the molecular level. (Review). Oncol Rep 10:1663–1682
5. Canizares F, Salinas J, de las Heras M, Diaz J, Tovar I, Martinez P, Penafiel R (1999) Prognostic value of ornithine decarboxylase and polyamines in human breast cancer: correlation with clinicopathologic parameters. Clinical Cancer Research 5:2035–2041
6. Canizares F, Salinas J, de las Heras M, Diaz J, Tovar I, Martinez P, Penafiel R (1999) Prgnostic value of ornithine decarboxylase and polyamines in human breast cancer: correlations with clinicopathological parameters. Clin Cancer Res 5:2035–2041
7. Casero RAJ, Celano P, Ervin SJ, Porter CW, Bergeron RJ, Libby PR (1989) Differential induction of spermidine/spermine N^1-acetyltransferase in human lung cancer cells by the bis(ethyl)polyamine analogues. Can Res 49:3829–3833
8. Chen Y, Kramer D, Jell J, Vujcic S, Porter CW (2003) siRNA suppression of polyamine analogue-induced spermidine/spermine N^1-acetyltransferase. Mol Pharm 64:1153–1159
9. Chen Y, Kramer DL, Li F, Porter CW (2003) Loss of inhibitor of apoptosis proteins as a determinant of polyamine-analogue-induced apoptosis in human melanoma cells. Oncogene 22:4964–4972
10. Devereux W, Wang Y, Stewart TM, Hacker A, Smith R, Frydman B, Valasinas AL, Reddy VK, Marton LJ, Ward TD, Woster PM, Casero RA (2003) Induction of the PAOh1/SMO polyamine oxidase by polyamine analogues in human lung carcinoma cells. Cancer Chemother Pharmacol 52:383–390
11. Di Francesco AM, Riccardi R (2002) Cellular and molecular aspects of the drugs of the future. Cell Mol Life Sci 59:1914–1927
12. Eisen MB, Spellman PT, Brown PO, Botstein D (1998) Cluster analysis and display of genome-wide expression patterns. Proc Natl Acad Sci USA 95:14863–14868
13. Hector S, Bolanowska-Higdon W, Zdanowicz J, Hitt S, Pendyala L (2001) In vitro studies on the mechanisms of oxaliplatin resistance. Cancer Chemother Pharmacol 48:398–406
14. Hector S, Hawthorn L, Greco W, Pendyala L (2002) Gene expression profiles after oxaliplatin treatment in A2780 ovarian carcinoma cells. Proc AACR 43:62
15. Hector S, Porter CW, Kramer DL, Clark K, Prey J, Kiesel N, Diegelman P, Chen Y, Pendyala L (2004) Polyamine catabolism in platinum drug action: Interactions between oxaliplatin and the polyamine analogue N^1, N^{11}-diethylnorspermine at the level of spermidine/spermine N^1-acetylransferase. Mol Cancer Ther 3:813–822
16. Kahana C, Asher G, Shaul Y (2005) Mechanisms of protein degradation. An odyssey with ODC. Cell Cycle 4:1461–1464
17. Kramer DL, Vujcic S, Diegelman P, Alderfer J, Miller JT, Black JD, Bergeron RJ, Porter CW (1999) Polyamine analogue induction of the p53-p21WAF1/CIP1-Rb pathway and G1 arrest in human melanoma cells. Can Res 59:1278–1286
18. Levasseur LM, Slocum HK, Rustum YM, Greco WR (1998) Modeling of the time-dependency of in vitro drug cytotoxicity and resistance. Cancer Res 58:5749–5761
19. Libby PR, Henderson M, Bergeron RJ, Porter CW (1989) Major increases in spermidine/spermine-N1-acetyltransferase activity by spermine analogues and their relationship to polyamine depletion and growth inhibition in L1210 cells. Cancer Res 49:6226–6231
20. Mangold U (2005) The antizyme family: polyamines and beyond. IUBMB Life 57:671–676
21. Mohan RR, Challa A, Gupta S, Bostwick DG, Ahmad N, Agarwal R, Marengo SR, Amini SB, Paras F, MacLennan GT, Resnick MI, Mukhtar H (1999) Overexpression of ornithine decarboxylase in prostate cancer and prostatic fluid in humans. Clin Cancer Res 5:143–147
22. Porter C, Herrera-Omelas L, Pera P, Petrelli NF, Mittleman A (1987) Polyamine biosynthetic activity in normal and neoplastic human colorectal tissues. Cancer 60:1275–1281
23. Porter CW, Bernacki RJ, Miller J, Bergeron RJ (1993) Antitumor activity of *N*1,*N*11-bis(ethyl)norspermine against human melanoma xenografts and possible biochemical correlates of drug action. Can Res 53:581–586
24. Porter CW, Ganis B, Libby PR, Bergeron RJ (1991) Correlations between polyamine analogue-induced increases in spermidine/spermine N^1-acetyltransferase activity, polyamine pool depletion, and growth inhibition in human melanoma cell lines. Cancer Res 51:3715–3720
25. Rubinstein LV, Shoemaker RH, Paull KD, Simon RM, Tosini S, et al (1990) Comparison of in vitro anticancer drug screening data generated with a tetrazolium assay versus a protein assay against a diverse panel of human tumor cell lines. J Nat Cancer Inst 82:1113–1118
26. Scalabrino G, Ferioli ME (1985) Degree of enhancement of polyamine biosynthetic decarboxylase activities in human tumors: A useful new index of degree of malignancy. Cancer Detect Prev 8:11
27. Shappell NW, Miller JT, Bergeron RJ, Porter CW (1992) Differential effects of the spermine analog, N^1,N^{12}-bis(ethyl)-spermine, on polyamine metabolism and cell growth in human melanoma cell lines and melanocytes. Anticancer Res 12:1083–1089
28. Thomas T, Thomas TJ (2001) Polyamines in cell growth and cell death: molecular mechanisms and therapetic applications. Cell Mol Life Sci 58:244–258
29. Thomas T, Balabhadrapathruni S, Gallo MA, Thomas TJ (2002) Development of polyamine analogs as cancer therapeutic agents. [Review]. Oncol Res 13:123–135
30. Tusher VG, Tibshirani R, Chu G (2001) Significance analysis of microarrays applied to the ionizing radiation response. [erratum appears in Proc Natl Acad Sci USA 2001 98(18):10515]. Proc Natl Acad Sci USA 98:5116–5121
31. Urdiales JL, Medina MA, Sanchez-Jimenez F (2001) Polyamine metabolism revisited. Eur J Gastroenter 13:1015–1019
32. Varma R, Hector S, Pendyala L, Greco WR (2005) Modeling and analysis of drug concentration-effect and time course patterns in gene expression data from microarray experiments. Proc AACR 46:2
33. Varma RR, Hector S, Clark K, Greco WR, Hawthorn L, Pendyala L (2005) Gene expression profiling of a clonal isolate of oxaliplatin resistant ovarian carcinoma cell line A2780/C10. Oncol Rep 14:925–932

34. Vujcic S, Diegelman P, Bacchi CJ, Kramer DL, Porter CW (2002) Identification and characterization of a novel flavin-containing spermine oxidase of mammalian cell origin. Biochem J 367:665–675
35. Vujcic S, Halmekyto M, Diegelman P, Gan G, Kramer DL, Janne J, Porter CW (2000) Effects of conditional overexpression of spermidine/spermine N^1-acetyltransferase on polyamine pool dynamics, cell growth, and sensitivity to polyamine analogs. J Biol Chem 275:38319–38328
36. Vujcic S, Liang P, Diegelman P, Kramer DL, Porter CW (2003) Genomic identification and biochemical characterization of the mammalian polyamine oxidase involved in polyamine back-conversion. Biochem J 370:19–28